2015

A Novel Ruminant Emission Measurement System: Part II. Commissioning

Guilherme D. N. Maia
Iowa State University

Brett C. Ramirez
Iowa State University, bramirez@iastate.edu

Angela R. Green
University of Illinois at Urbana-Champaign

Yi Sun
University of Illinois at Urbana-Champaign

Luis F. Rodríguez
University of Illinois at Urbana-Champaign

See next page for additional authors

A Novel Ruminant Emission Measurement System: Part II. Commissioning

Abstract
The Ruminant Emission Measurement System (REMS) supports research on the relationships between bovine nutrition, genetics, and management strategies by measuring eructated CH_4 emissions from ruminal activity. Part I of this series provides the description and design evaluation of the newly developed REMS using uncertainty analysis tools. Part II of this series describes REMS commissioning and documents the whole system and subsystem performance. Subsystem assessments included verification of chamber positive pressurization, thermal environmental control performance, and integrity of the gas sampling system. Integrity of the entire system was verified through a steady-state mass recovery percent (SSMRP) analysis, which compared the total mass measured by REMS (mass recovered) to the total mas injected from a certified reference (mass injected) during steady-state operation. Uncertainty analysis conducted as a part of commissioning included propagation of instrument uncertainties, quantification of the variability in repeated tests, and identification of systematic errors. Results from the subsystem evaluation verified that chambers were positively pressurized, maintained thermal environmental comfort, and resulted in no measurable leakage along the sampling path from the chamber to the gas analyzer. The mean SSMRP for the six chambers ranged from 92.0% to 96.6% with absolute expanded uncertainties (~95% confidence interval) ranging from 10.4% to 13.0%. Mass recovered uncertainty contributed from 70.1% to 90.7% to SSMRP uncertainty, mass injected uncertainty contributed from 2.5% to 4.0%, and reproducibility contributed from 5.6% to 27.3%. Significant ($p < 0.05$) SSMRP systematic bias was found for most chambers; therefore, correction for bias following the methods developed here is recommended. Example measurements from REMS research demonstrate how to incorporate a documented standard uncertainty for emissions.

Keywords
Cattle, Climate change, Food security, Methane production, Uncertainty

Disciplines
Agriculture | Bioresource and Agricultural Engineering | Climate

Comments
This article is published as Maia, Guilherme D. N., Brett C. Ramirez, Angela R. Green, Yi Sun, Luis F. Rodriguez, Daniel W. Shike, and Richard S. Gates. "A novel ruminant emission measurement system: Part II. Commissioning." *Transactions of the ASABE* 58, no. 6 (2015): 1801-1815. DOI: 10.13031/trans.58.10753. Posted with permission.

Authors
Guilherme D. N. Maia, Brett C. Ramirez, Angela R. Green, Yi Sun, Luis F. Rodríguez, Daniel W. Shike, and Richard S. Gates

A NOVEL RUMINANT EMISSION MEASUREMENT SYSTEM: PART II. COMMISSIONING

G. D. N. Maia, B. C. Ramirez, A. R. Green, Y. Sun, L. F. Rodriguez, D. W. Shike, R. S. Gates

ABSTRACT. *The Ruminant Emission Measurement System (REMS) supports research on the relationships between bovine nutrition, genetics, and management strategies by measuring eructated CH_4 emissions from ruminal activity. Part I of this series provides the description and design evaluation of the newly developed REMS using uncertainty analysis tools. Part II of this series describes REMS commissioning and documents the whole system and subsystem performance. Subsystem assessments included verification of chamber positive pressurization, thermal environmental control performance, and integrity of the gas sampling system. Integrity of the entire system was verified through a steady-state mass recovery percent (SSMRP) analysis, which compared the total mass measured by REMS (mass recovered) to the total mas injected from a certified reference (mass injected) during steady-state operation. Uncertainty analysis conducted as a part of commissioning included propagation of instrument uncertainties, quantification of the variability in repeated tests, and identification of systematic errors. Results from the subsystem evaluation verified that chambers were positively pressurized, maintained thermal environmental comfort, and resulted in no measurable leakage along the sampling path from the chamber to the gas analyzer. The mean SSMRP for the six chambers ranged from 92.0% to 96.6% with absolute expanded uncertainties (~95% confidence interval) ranging from 10.4% to 13.0%. Mass recovered uncertainty contributed from 70.1% to 90.7% to SSMRP uncertainty, mass injected uncertainty contributed from 2.5% to 4.0%, and reproducibility contributed from 5.6% to 27.3%. Significant ($p < 0.05$) SSMRP systematic bias was found for most chambers; therefore, correction for bias following the methods developed here is recommended. Example measurements from REMS research demonstrate how to incorporate a documented standard uncertainty for emissions.*

Keywords. *Cattle, Climate change, Food security, Methane production, Uncertainty.*

Part I of this series (Maia et al., 2015) introduced the design evaluation and description of the Ruminant Emission Measurement System (REMS), which consists of six positive-pressure ventilated hood-type respiration chambers. The objective of REMS is to support research on the relationships between bovine nutrition, genetics, and management strategies by measuring eructated methane (CH_4) emissions from ruminal activity. The evaluation performed in Part I documented a systematic methodology to estimate combined standard uncertainty associated with calculated CH_4 emissions from ruminant eructation. An analytical approach to the design analysis was critical to assess the contributions of individual parameter uncertainties and their effects on the emission rate (ER) uncertainty. Knowledge of uncertainty is critical to compare ruminant emission measurement techniques (i.e., sulfur hexafluoride (SF_6) tracer or *in vitro* gas production technique) or different chamber systems to provide expected confidence levels for the measurements reported.

In addition to the analytical approach applied to REMS design in Part I, commissioning of the system after construction is required to verify performance and compare that performance to the design assumptions and analysis, as well as to evaluate integrity of the physical system. Commissioning is the final step before full implementation and includes information associated with REMS operation, identification of systematic errors, and quantification of variability over repeated tests. A mass recovery analysis can serve as a "whole-system calibration" or as a check on operation integrity. These are crucial steps in the evolution of open-circuit systems for livestock emissions measurement.

The mass recovery test compares a known amount of mass injected (reference) into the chamber to the total mass measured by the system, and it has been the primary method to validate the chamber technique (McLean and Tobin, 1987). Several approaches have been used to evaluate system recovery. The alcohol combustion method (Carpenter and Fox, 1923) utilizes stoichiometric relationships of the combustion of alcohols to determine mass generated, but it

Submitted for review in April 2014 as manuscript number PAFS 10753; approved for publication by the Plant, Animal, & Facility Systems Community of ASABE in August 2015.

The authors are **Guilherme D. N. Maia, ASABE Member,** Post-Doctoral Research Assistant, and **Brett C. Ramirez, ASABE Member,** Graduate Research Assistant, Department of Agricultural and Biosystems Engineering, Iowa State University, Ames, Iowa; **Angela R. Green, ASABE Member,** Assistant Professor, **Yi Sun, ASABE Member,** Graduate Research Assistant, and **Luis F. Rodríguez, ASABE Member,** Associate Professor, Department of Agricultural and Biological Engineering, University of Illinois Urbana-Champaign, Urbana, Illinois; **Daniel W. Shike,** Assistant Professor, Department of Animal Sciences, University of Illinois Urbana-Champaign, Urbana, Illinois; **Richard S. Gates, ASABE Fellow,** Professor, Department of Agricultural and Biological Engineering, University of Illinois Urbana-Champaign, Urbana, Illinois. **Corresponding author:** Guilherme D. N. Maia, AESB MC-644, 1304 W. Pennsylvania Ave., Urbana, IL 61801; phone: 859-608-7570; e-mail: gdnmaia@gmail.com.

Vol. 58(6): 1801-1815 ISSN 2151-0032 DOI 10.13031/trans.58.10753

is often difficult to determine whether the full combustion of the alcohol actually occurred (McLean and Tobin, 1987). Recently, more accurate mass recovery tests have used pulse injections of a known volume of gas and by continuous or step injection of a known mass flow (Hellwing et al., 2012; Klein and Wright, 2006; Pinares-Patiño et al., 2011; Suzuki et al., 2007). A number of precise measurements are required to accurately quantify the known mass entering the system, for example, input gas (e.g., CH_4, CO_2, and H_2S) controlled by a mass flow controller or determined gravimetrically as the change in weight of an open gas cylinder on a scale. Errors during the determination of the injected mass may lead to incorrect estimates of mass recovered and should be included in the final stated uncertainty. A mass recovery test provides insights about the dynamics of the chamber and the integrity of the sampling system. Limited work is available on error analysis and methodology for the injected mass, along with an analytical approach to determine the system time constant applied to the chamber technique (McGinn, 2006). More descriptive calibration procedures are available in other disciplines, e.g., for soil carbon flux measurement chambers (McGinn, 2006). A mass recovery test reported without quantification of the injected and recovered masses standard uncertainties reduces confidence in emissions measurement.

The main goal of this work was to introduce and describe a systematic methodology to commission REMS (full description of the system is available in Part I; Maia et al., 2015). In the commissioning phase, the operation of each subsystem of REMSs was assessed, followed by a mass recovery whole-system validation. In addition, this analysis determined systematic errors and combined uncertainty related to a reference mass of tracer gas injected into the system, which was a new input, not assessed in Part I. To achieve these goals, the following objectives were completed:

1. Subsystem performance validation prior to whole-system evaluation.
2. Whole-system evaluation, subdivided into four procedures:
   a) Chamber system dynamics, in order to determine the time to reach steady-state fresh air exchange rate.
   b) Quantification of mass recovered of a reference tracer gas (SF_6) during steady-state operation.
   c) Determination of combined standard uncertainty associated with the mass recovery and assessment of individual contributions to the mass recovery standard uncertainty.
   d) Evaluation of systematic errors during whole-system assessment and application of bias correction.

This commissioning analysis fulfills the need to establish and document a procedure quantifying uncertainty of emissions measured with REMS. This procedure also applies to other respiration chambers and indirect calorimeter systems in operation, or to future designs.

.

MATERIALS AND METHODS

REMS OVERVIEW

REMS was installed in six metabolism stalls at the University of Illinois at Urbana-Champaign Beef and Sheep Field Facility and consists of four major subsystems: (1) six identical positive-pressure ventilated hood chambers (VHC), (2) an individual thermal environmental control subsystem (TECS) for each chamber, (3) a fresh air supply and measurement subsystem (FASMS), and (4) a gas sampling subsystem (GSS). A description of the operation and a set of schematics of REMS are provided in Part I (Maia et al., 2015). Details of the FASMS, including design, construction, and validation, can be found elsewhere (Ramirez, 2014; Ramirez et al., 2014).

SUBSYSTEM VALIDATION

Individual subsystems were assessed for proper function initially in the commissioning. Detailed protocols for system maintenance and testing are documented in a systematic standard operating procedure (Sun, 2013). All experiments using animals were approved by the University of Illinois at Urbana-Champaign Institutional Animal Care and Use Committee (IACUC) under Protocol No. 11214.

Ventilated Hood Chamber Pressure Distribution

Positive pressurization was required over the entire internal volume of the VHCs to ensure no background gas infiltration could dilute the sample. Fifteen static pressure measurements were collected inside each of the six VHCs at five locations and three heights (fig. 1). A fresh air ventilation rate of 481 ±0.1 L min^{-1} (17 ±0.0035 cfm), was selected as the expected flow during experiments and was used during all tests. The canvas hood was cinched during the test to create a similar situation as observed during preliminary animal testing. An electronic differential manometer (model 260-MS4, Setra, Boxborough, Mass.) was used to map chamber static pressure with respect to the room. A pressure buffer was attached to the end of the high-pressure port tube to reduce disturbances from turbulent air in the

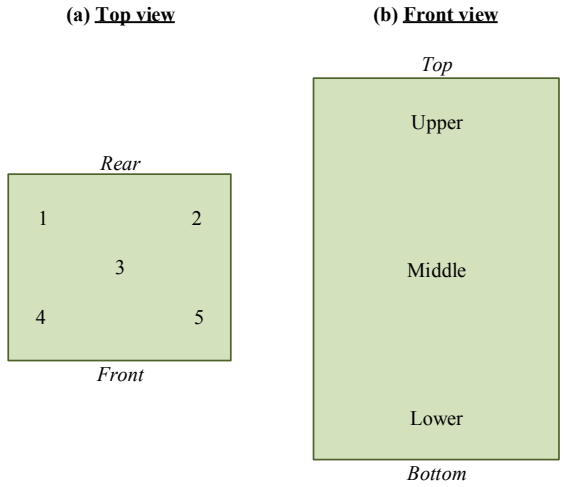

Figure 1. Static pressure sampling locations and heights: (a) top view showing the five sampling locations per height in the chamber and (b) front view showing the three sampling heights (upper, middle, and lower).

chamber. Results were reported as the average of each sample location across the three heights, and the average of the five cross-section sample locations for each of the three heights (fig. 2). A smoke test was performed to visually confirm positive pressurization, flow patterns, and gas mixing. A smoke stick (S102, Regin HVAC Products, Inc., Oxford, Conn.) with 45 s burn-time and volume generation capacity of 4.25 m^3 (150 ft^3) was initially placed inside the feeding bin (bottom of the chamber), then around the outside of the chamber, and lastly in the canvas hood.

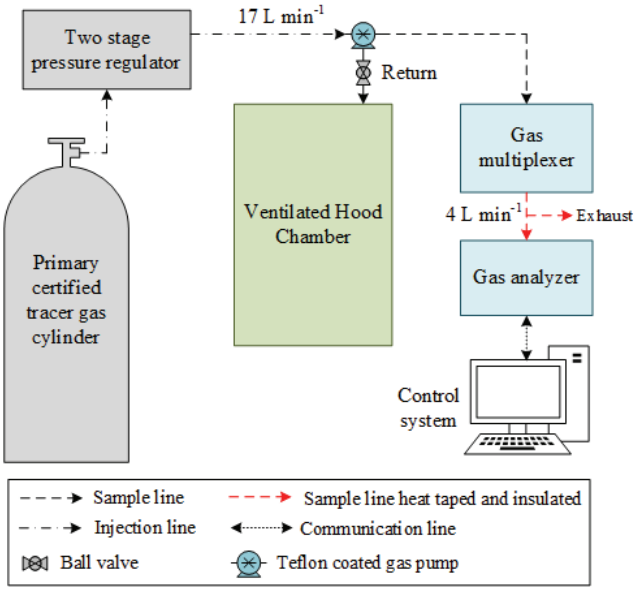

Figure 2. Configuration of gas sampling subsystem integrity test for one chamber. The sampling line was disconnected from the sampling port at the top of the chamber and connected to the outlet of a tracer gas cylinder. FASMS, TECS, and other GSS components are omitted for clarity. The same procedure and configuration were used for each of the six chambers.

Thermal Environment Performance

A 23 h test with six steers (826 ±64 kg; one steer per chamber) was conducted to evaluate the ability of TECS to maintain set point temperature, remove moisture, and assess the potential for condensation. Humidity ratio and dew point temperature were used as the thermal environment assessment parameters and were calculated for dry-bulb temperature and relative humidity measurements recorded every 43 s over the duration of the test. Animals were provided *ad libitum* food and water.

Gas Sampling Subsystem Integrity

Leakage along the gas sampling path (which contains multiple connections that are subject to potential leakage) from the sampling port can provide false, diluted gas concentration measurements. The GSS integrity was evaluated by supplying a constant flow of SF_6 at a known concentration to the gas sampling port of each VHC and noting the concentration recorded at the gas analyzer (fig. 2; eq. 1). The supplied SF_6 concentration was 6.235 ±0.004 ppm_v (mean ±SD), which was the actual concentration measured by the gas analyzer when the primary certified tank of SF_6 was directly connected to the gas analyzer (flow of approximately 4 L min^{-1}) using a single connection free of leakage. The gas analyzer optical filter configuration and sam-

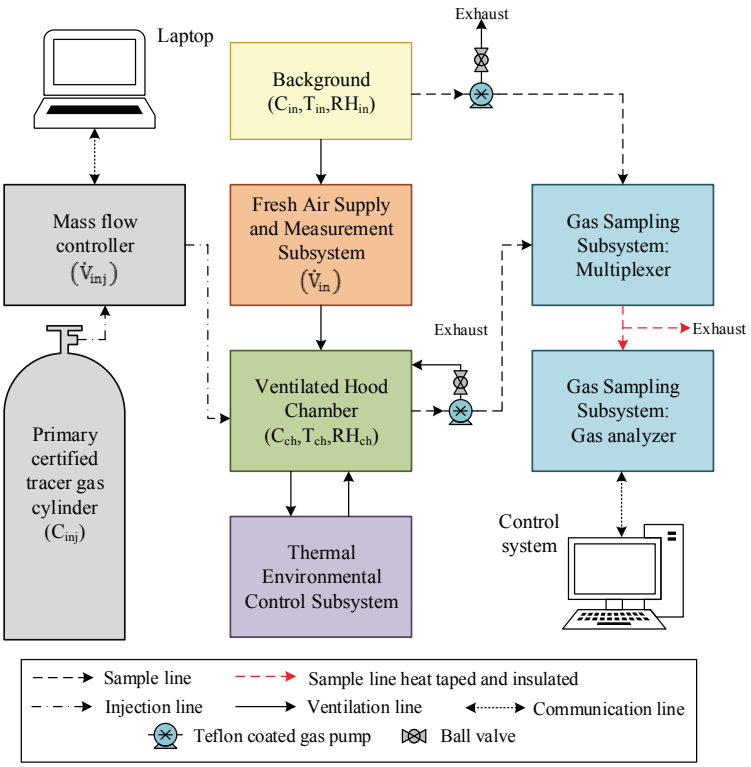

Figure 3. Experimental setup for steady-state mass recovery test in one chamber. Tracer gas (C_{inj}) was supplied at a constant volumetric flow rate ($\dot{V}_{inj}$) from a mass flow controller. Mass recovered was determined from temperature (T_{in}, T_{ch}), relative humidity (RH_{in}, RH_{ch}), gas concentration (C_{in}, C_{ch}), and ventilation rate ($\dot{V}_{in}$) measurements in REMS.

pling integration time followed the same setup reported in Part I (Maia et al., 2015). The solenoid array in the gas multiplexer was independently tested and found to have no leaks prior to GSS integrity test (Sun, 2013):

$$\text{GSSR} = \frac{C_{measured}\,(\text{full sampling line})}{C_{target}\,(\text{calibration})} \times 100 \qquad (1)$$

where

GSSR = gas sampling subsystem recovery (%)

$C_{measured}$ = measured gas concentration (ppm_v)

C_{target} = target gas concentration determined from post-calibration check (6.235 ppm_v).

Steady-State Mass Recovery Test

A steady-state mass recovery test (SSMRT) was developed to provide a whole-system evaluation for one chamber at a time. The SSMRT consisted of injecting a known mass (reference) and comparing it to the mass measured by REMS. This approach is useful to verify system performance and identify potential problems that might have developed, such as leaks or failed components (McLean and Tobin, 1987).

EXPERIMENTAL SETUP

Mass Flow Injected

A SSMRT was performed individually in each of the six chambers with eight replicates (n = 8) over time for each chamber. The mass flow injected into the system was supplied by a primary certified tank containing 3929 ppm_v (first four replicates) and 3947 ppm_v (last four replicates) of SF_6 (tracer gas) balanced with N_2 (Airgas, Inc., Bowling Green, Ky.) connected to a mass flow controller (MFC) (Series 4040, Environics, Tolland, Conn.) and set to inject a constant flow rate of 4 L min^{-1} (fig. 3).

Mass Flow Recovered

REMS was set to operate as if an animal were present in the chamber, with the TECS and FASMS operating and the feed bin in place. Dry-bulb temperature and relative humidity from the background (incoming ventilation) and mixed chamber gas were recorded simultaneously with each gas concentration measurement during steady-state conditions. Fresh air ventilation was set at a constant rate for each SSMRT and ranged from 479.1 to 525.1 L min^{-1} (16.9 to 18.6 cfm) for all chambers and replicates, which was the calculated ventilation rate required for control of moisture, temperature, and CO_2 with one animal in the chamber for a cattle weight range of 230 to 1000 kg. Gas analyzer optical filter configuration and sampling integration time were set as reported in Part I (Maia et al., 2015). The outlet tube from the MFC was placed where the TECS recirculation supply and FASMS supply air streams mixed to ensure thorough mixing of the injected gas. The canvas hood located in the back of the chamber was cinched around a 38.1 cm (15 in.) diameter plastic pipe. The inside area of the pipe was sealed, and a 103 cm^2 (16 $in.^2$) section was removed to create a small opening serving as a conservative representation of the leakage around the animal's neck. This procedure was verified to not affect positive pressurization of the chamber (Sun, 2013). Prior to gas injection, five consecutive background gas concentrations were measured at the ventilation inlet, followed by five additional background measurements inside the chamber (fig. 4). During tracer gas injection, 12 consecutive measurements collected at steady-state were used to determine REMS mass flow recovered. Finally, after all chamber samples were collected, ten additional background concentrations were recorded and averaged with the first ten recorded background concentrations (prior to injection) to establish a mean background concentration (fig. 4).

Steady-State Determination

The system time constant was determined for each VHC from the time series recording of tracer gas injection. The time constants then served as a metric to determine the time to reach steady-state using five time constants (≅ 99% of steady-state; fig. 4). The time constant was determined assuming that the gas concentrations in each VHC acted as a

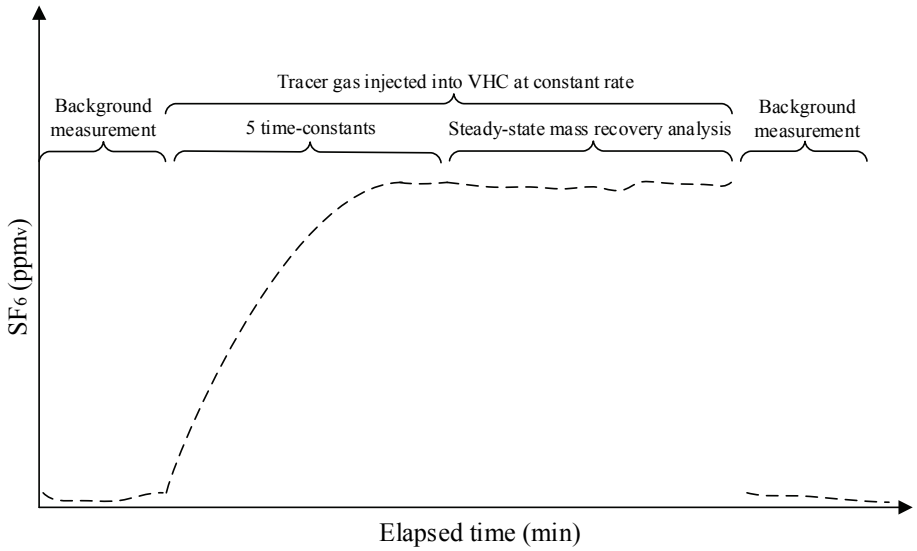

Figure 4. The system was considered to be at steady-state after five system time constants. The recovery test procedure measured background concentration first, allowed the chamber to reach steady-state, and concluded with additional background measurement.

first-order system (Zhang, 2005). Thus, this initial value problem (eq. 2) can be written as:

$$C(t) = C_s + (C_0 - C_s)e^{-\frac{t}{\tau}} \quad (2)$$

where

$C(t)$ = tracer gas concentration as a function of time (ppm_v)

C_s = steady-state tracer gas concentration (ppm_v)

C_o = incoming tracer gas concentration (ppm_v)

t = time (min)

τ = system time constant (min^{-1}).

The regression parameters (C_s, C_o, and τ) were estimated from a nonlinear regression of tracer gas concentrations versus elapsed time using the software package Origin-Pro 9 (OriginLab, Northampton, Mass.).

STEADY-STATE MASS RECOVERY ANALYSIS

The measurement parameters described in the experimental setup were used in the analysis of the ratio of mass recovered to mass injected. When expressed on a percent basis, this ratio determines the steady-state mass recovery percent (SSMRP). The total mass injected and recovered was obtained from the integration of the individual mass flow measurements collected over the steady-state period. The mass flow recovery equation was obtained from a derivation of a tracer gas component mass balance (with VHC chamber as the control volume) at steady-state, while the mass flow injected equation was a function of the volumetric flow and tracer gas cylinder concentration.

Reference Mass Injected

Mass flow injected was calculated from the measured injected volumetric flow rate and tracer gas concentration at steady-state:

$$\dot{m}^{inj} = \dot{V}_{inj} \times C_{inj} \times \frac{M \cdot p_{std}}{R \cdot T_{std}} \times 10^{-6} \quad (3)$$

where

$\dot{m}^{inj}$ = mass flow injected ($g\ h^{-1}$)

$\dot{V}_{inj}$ = injected volumetric flow rate ($m^3\ s^{-1}$)

C_{inj} = injected gas concentration (ppm_v)

M = molecular mass of gas (146.06 kg mol^{-1})

R = universal constant of ideal gases (8.314 m^3 Pa K^{-1} mol^{-1})

T_{std} = standard temperature (273.15 K)

P_{std} = standard pressure (101325 Pa).

The integration of mass flow injected over the steady-state interval yields the total mass of tracer gas injected:

$$m^{inj} = \sum_{i=1}^{n} t_i \times \dot{m}_i^{inj} \quad (4)$$

where

n = number of steady-state measurements

m^{inj} = total tracer gas mass injected by the reference (g)

t_i = time at steady-state measurement (h).

Because the tracer gas injection rate was constant, the area under the curve (mass flow rate versus time) is simply the product of the mass flow rate injected and the duration of the steady-state test.

Mass Recovered

The moist air mass flow balance previously presented in Part I (Maia et al., 2015; eq. 1) requires an additional input due to the non-negligible mass contribution of the injected tracer gas mixture. Including the injected tracer gas flow rate, the moist air mass flow balance (eq. 5) becomes:

$$\dot{V}_{ex}^{rec} = \dot{V}_{in} \times \left(\frac{\rho_{in}^{ma}}{\rho_{ex}^{ma}} \right) + \dot{V}_{inj} \times \left(\frac{\rho_{inj}^{cyl}}{\rho_{ex}^{ma}} \right) \quad (5)$$

where

$\dot{V}_{ex}^{rec}$ = exhaust volumetric flow rate ($m^3\ s^{-1}$)

$\dot{V}_{in}$ = incoming air flow rate ($m^3\ s^{-1}$)

ρ_{in}^{ma} = incoming moist air density (kg dry air m^{-3} moist air)

ρ_{ex}^{ma} = exhaust moist air density (kg dry air m^{-3} moist air)

$\dot{V}_{inj}$ = injected tracer gas flow rate ($m^3\ s^{-1}$)

ρ_{inj}^{cyl} = dry density of the injected tracer gas at standard conditions (273.15 K and 101325 Pa) (6.52 kg dry mixture m^{-3} mixture volume).

The second term on the right side of equation 5 accounts for tracer gas injection. Density of the tracer gas mixture (eq. 6) was determined as follows:

$$\rho_{inj}^{cyl} = y_{N_2} \times \rho_{N_2}^{std} + y_{SF_6} \times \rho_{SF_6}^{std} \quad (6)$$

where

y_{N_2} = mole fraction of N_2 in the cylinder (dimensionless)

$\rho_{N_2}^{std}$ = dry densities of N_2 at standard conditions (1.25 kg dry mixture m^{-3} mixture dry volume).

y_{SF_6} = mole fraction of SF_6 in the cylinder (dimensionless)

$\rho_{SF_6}^{std}$ = dry densities of SF_6 at standard conditions (6.17 kg dry mixture m^{-3} mixture dry volume).

A gas mass flow balance similar to that derived in Part I (Maia et al., 2015; eq. 2) was used in the SSMRP analysis with one modification: substitution of the exhaust volumetric flow rate ($\dot{V}_{ex}^{rec}$) from equation 5, which accounts for the addition of the injected mass flow of the tracer gas into the chamber. The difference between the exhaust mass flow rate and the incoming mass flow rate ($\dot{m}_{in}^{gas}$) produces the following mass recovery rate eq. (eq. 7):

$$\dot{m}^{rec} = \left[\left(\dot{V}_{in} \frac{\rho_{in}^{ma}}{\rho_{ex}^{ma}} + \dot{V}_{inj} \frac{\rho_{inj}^{cyl}}{\rho_{ex}^{ma}} \right) \times \frac{C_{ch}}{T_{ch}} - \left(\dot{V}_{in} \frac{C_{in}}{T_{in}} \right) \right] \times 10^{-6} \frac{M \cdot P_b}{R} \quad (7)$$

where

$\dot{m}^{rec}$ = recovered gas mass flow (g h^{-1})
C_{ch} = chamber gas concentration (ppm$_v$)
C_{in} = incoming background gas concentration (ppm$_v$)
T_{in} = chamber dry-bulb temperature (K)
T_{ch} = incoming background dry-bulb temperature (K)
M = molecular mass of gas (g mol^{-1})
p_b = local barometric pressure (98.639 kPa) (ASHRAE, 2013).

In Part I (Maia et al., 2015; eqs. 2 and 3), the difference between the exhaust gas mass flow and incoming gas mass flow was equal to the generated gas mass flow, which provides the animal emission rate: $\mathrm{ER} = \dot{m}_{gen}^{gas} = \dot{m}_{ex}^{gas} - \dot{m}_{in}^{gas}$. Here, the difference produces the mass flow recovered ($\dot{m}^{rec} = \dot{m}_{ex}^{gas} - \dot{m}_{in}^{gas}$) instead (eq. 7).

The total mass recovered (eq. 8) was determined by trapezoidal integration of the mass flow over the steady-state period:

$$m^{rec} = \sum_{i=1}^{n-1} \frac{1}{2}\left(t_{i+1} - t_i\right) \times \left(\dot{m}_i^{rec} + \dot{m}_{i+1}^{rec}\right) \tag{8}$$

where
n = number of steady-state measurements
m^{rec} = total tracer gas mass recovered by REMS (g)
t = time at steady-state measurement i (h).

The input parameters for this test included incoming and chamber temperatures, moist air densities, and tracer gas concentrations.

Steady-State Mass Recovery

The ratio of the mass recovered by REMS (eq. 8) to the mass injected by the reference (eq. 4) was defined as the SSMRP (eq. 9):

$$\mathrm{SSMRP} = \left(\frac{m^{rec}}{m^{inj}}\right) \times 100 \tag{9}$$

where SSMRP is the steady-state mass recovery percent (%).

UNCERTAINTY ANALYSIS OF STEADY-STATE MASS RECOVERY

The steady-state mass recovery percent standard uncertainty is determined from the propagation of standard uncertainties (ISO/IEC, 2008; Taylor and Kuyatt, 1994) from input measurements to mass recovered (eq. 8) and mass injected (eq. 4). The standard uncertainty (Δ) of each parameter is the associated best estimate of combined measurement error and is obtained with a truncated first-order Taylor series approximation applied to equations 3 and 7 assuming independent measurements (Jordan, 1991; Gates, 1994; Gates et al., 2009). The following sections characterize additional uncertainties associated with the commissioning of the system and include uncertainty analyses for the reference mass injected (mass flow and total mass), mass recovered (total mass), and SSMRP reproducibility. Parameter standard uncertainties associated with mass flow recovered temperature, relative humidity, moist air density, ventilation rate, and gas concentration are described elsewhere (Maia et al., 2015; Ramirez et al., 2014). A normal distribution (divisor = 1; C.I. ≈ 68%) or a rectangular distribution (divisor = √3; C.I. ≈ 68%) was applied to associated instrument uncertainties as appropriate (Taylor and Kuyatt, 1994).

Reference Mass Injected

The tracer gas mass flow injected uncertainty (eq. 10) was the combination of three primary sources of uncertainty, including tracer gas concentration, injection mass flow, and gas density:

$$\Delta\dot{m}^{inj} = \sqrt{\left(\frac{\partial \dot{m}^{inj}}{\partial C_{inj}}\Delta C_{inj}\right)^2 + \left(\frac{\partial \dot{m}^{inj}}{\partial \dot{V}_{inj}}\Delta \dot{V}_{inj}\right)^2 + \left(\frac{\partial \dot{m}^{inj}}{\partial \rho_{inj}^{cyl}}\Delta \rho_{inj}^{cyl}\right)^2} \tag{10}$$

where
$\Delta\dot{m}^{inj}$ = tracer mass flow injected standard uncertainty (g h^{-1})
ΔC_{inj} = tracer gas concentration standard uncertainty (ppm$_v$)
$\Delta\dot{V}_{inj}$ = tracer injected flow rate standard uncertainty (m^3 s^{-1})
$\Delta\rho_{inj}^{cyl}$ = injected tracer gas mixture density standard uncertainty (kg m^{-3}).

Tracer gas concentration standard uncertainty (eq. 11) was based on the primary certified tolerance specified by the manufacturer (Airgas, Inc., Bowling Green, Ky.) and the concentration uncertainty of the MFC accuracy. A rectangular distribution was assumed for these two sources of uncertainty:

$$\Delta C_{inj} = \sqrt{\left(\frac{\mathrm{MFCA} \times \mathrm{SP}}{\sqrt{3}}\right)^2 + \left(\frac{\mathrm{PCT} \times \mathrm{CV}}{\sqrt{3}}\right)^2} \tag{11}$$

where
MFCA = mass flow controller accuracy (±1% of the set point)
SP = set point for CV (ppm$_v$).
PCT = primary certified tolerance (±1% of the certified value)
CV = certified value (ppm$_v$).

The injected tracer gas flow rate had three major sources of uncertainty (eq. 12): calibration reference standard error obtained from the manufacturer's National Institute of Standards and Technology (NIST) traceable calibration (normal distribution), repeatability of the measurements (rectangular distribution), and reading resolution (rectangular distribution):

$$\Delta \dot{V}_{inj} = \sqrt{\left(\frac{\mathrm{CRSEx}}{1}\right)^2 + \left(\frac{\mathrm{Rep}}{\sqrt{3}}\right)^2 + \left(\frac{\mathrm{Res}}{\sqrt{3}}\right)^2} \tag{12}$$

where
CRSEx = calibration reference standard error (3.63E-07 m^3 s^{-1}; normal distribution)
Rep = repeatability (0.0005·SP m^3 s^{-1}; rectangular distri-

bution)

Res = resolution (1.67E-11 m^3 s^{-1}; rectangular distribution).

Tracer gas mixture density standard uncertainty (eq. 13) was defined from the combined contribution of uncertainty in molar fractions of constituents in the mixture:

$$\Delta\rho_{inj}^{cyl} = \sqrt{\left(\frac{\partial\rho_{inj}^{cyl}}{\partial y_{N_2}}\Delta y_{N_2}\right)^2 + \left(\frac{\partial\rho_{inj}^{cyl}}{\partial y_{SF_6}}\Delta y_{SF_6}\right)^2} \quad (13)$$

where

Δy_{N_2} = molar fraction of nitrogen (dimensionless; ±1% relative; rectangular distribution)

Δy_{SF_6} = molar fraction of sulfur hexafluoride (dimensionless; ±1% relative; rectangular distribution).

The mass injected standard uncertainty (eq. 14) was determined as follows:

$$\Delta m^{inj} = \sqrt{\left[(t_n - t_1)\times\Delta\dot{m}^{inj}\right]^2} \quad (14)$$

where

n = number of steady-state measurements

Δm^{inj} = tracer gas mass injected by the reference standard uncertainty (g)

$\Delta\dot{V}_{inj}$ = injected flow rate standard uncertainty (m^3 s^{-1})

ΔC_{inj} = injected tracer gas concentration standard uncertainty (ppm_v).

Mass Recovered

The standard uncertainty of mass recovered (eq. 15) can be written as:

$$\Delta m^{rec} = \sqrt{\sum_{i=1}^{n-1}\left[\frac{1}{2}(t_{i+1} - t_i)\times\left(\Delta\dot{m}_i^{rec} + \Delta\dot{m}_{i+1}^{rec}\right)\right]^2} \quad (15)$$

where

n = number of steady-state measurements

Δm^{rec} = total tracer gas mass recovered by REMS standard uncertainty (g)

$\Delta\dot{m}_i^{rec}$ = mass flow recovered standard uncertainty (g h^{-1}).

Reproducibility

Reproducibility (eq. 16) of SSMRP was the variability of the replicated measurements in time (n = 8) obtained over a one-year period (Taylor and Kuyatt, 1994):

$$\mathrm{Rep}_c = \sqrt{\frac{1}{n-1}\sum_{r=1}^{n}\left(\mathrm{SSMRP}_{c,r} - \overline{\mathrm{SSMRP}}_c\right)^2} \quad (16)$$

where

Rep_c = reproducibility of SSMRP for the c^{th} chamber (%)

n = number of replicates (n = 8)

c = chamber {1,…, 6}

r = replicate {1,…, 8}

$\mathrm{SSMRP}_{c,r}$ = steady-state mass recovery percent for the c^{th} chamber and r^{th} replicate (%)

$\overline{\mathrm{SSMRP}}_c$ = mean steady-state mass recovery percent for the c^{th} chamber (%).

Changes in conditions for the reproducibility test included the personnel taking the measurements, time and day of the measurements, and changes in indoor and outdoor environmental conditions.

Steady-State Mass Recovery Percent

Finally, the SSMRP uncertainty (eq. 17) was obtained by combining the standard uncertainties associated with the mass injected, mass recovered, and SSMRP analysis reproducibility:

$$\Delta\mathrm{SSMRP}_{c,r} = \sqrt{\left(\frac{\partial\mathrm{SSMRP}_{c,r}}{\partial m_{c,r}^{inj}}\Delta m_{c,r}^{inj}\right)^2 + \left(\frac{\partial\mathrm{SSMRP}_{c,r}}{\partial m_{c,r}^{rec}}\Delta m_{c,r}^{rec}\right)^2 + (\mathrm{Rep}_c)^2} \quad (17)$$

where ΔSSMRP is the steady-state mass recovery percent standard uncertainty (%).

A coverage factor of 2 (k = 2) was applied to the SSMRP standard uncertainty in order to expand the confidence interval to approximately 95%. Relative standard uncertainty was also expanded following the same coverage factor. Table 1 summarizes the sources of uncertainties used to calculate ΔSSMRP.

SYSTEMATIC BIAS ANALYSIS

Test for Significance

For each chamber, the SSMRPs and their standard uncertainties calculated from the replicated SSMRT were used to determine if the mean SSMRP was significantly different from the hypothetical mean of 100% mass recovered. If so, this would indicate that a bias existed in the mass recovered measurement for each chamber.

Let the mean SSMRP for each chamber be an independent normal random variable with an unknown population mean, and let the best estimate of population variance be the square of the mean standard uncertainty of SSMRP. The mean standard uncertainty of SSMRP was calculated as follows:

$$\Delta\overline{\mathrm{SSMRP}}_c = \frac{1}{n}\sqrt{\sum_{r=1}^{n}\left(\Delta\mathrm{SSMRP}_{c,r}\right)^2} \quad (18)$$

where $\Delta\overline{\mathrm{SSMRP}}_c$ is the mean standard uncertainty of SSMRP (%).

Equation 19 provides the basis for a hypothesis test for whether a significant systematic bias exists. For no bias, $\overline{\mathrm{SSMRP}}_c$ for each chamber would be 100%. Assuming that $\overline{\mathrm{SSMRP}}_c$ is distributed according to the Student t-distribution with standard error given by equation 18, then:

$$t_c^{calc} = \frac{\overline{\mathrm{SSMRP}}_c - 100}{\Delta\overline{\mathrm{SSMRP}}_c} \quad (19)$$

is distributed according to the Student t-distribution with mean zero and unity variance, with $n - 1$ (= ν = 7) degrees of freedom. The test for significance was two-sided.

Table 1. Summary from instrument and parameter error analysis used to determine standard uncertainty associated with mass flow recovered, mass flow injected, and steady-state mass recovery percent.

Symbol	Unit	Description	Source of Uncertainty	Manufacturer	Source
ΔT_{in}, ΔT_{ch}	K	Dry-bulb temperature	T/RH sensor	Vaisala, HMP60-L, Helsinki, Finland	Ramirez et al., 2014
ΔRH_{in}, ΔRH_{ch}	%	Relative humidity	T/RH sensor	Vaisala, HMP60-L, Helsinki, Finland	Ramirez et al., 2014
$\Delta \dot{V}_{in}$	$m^3\ s^{-1}$	Incoming flow rate	Orifice meter	Custom	Ramirez et al., 2014
$\Delta \rho_{in}^{ma}$, $\Delta \rho_{ch}^{ma}$	kg m^{-3}	Moist air density	Equation 2-16 (Albright, 1990)	-	Ramirez et al., 2014
ΔC_{in}, ΔC_{ch}	ppm_v	Gas concentration	Infrared photoacoustic multi-gas analyzer	Innova 1412, LumaSense Technologies, Inc., Santa Clara, Cal.	Maia et al., 2015
$\Delta \dot{V}_{inj}$	$m^{-3}\ s^{-1}$	Injected flow rate	Mass flow controller	Series 4040, Environics, Tolland, Conn.	Equation 12
ΔC_{inj}	ppm_v	Tracer gas concentration	Primary certified cylinder	Airgas, Inc., Bowling Green, Ky.	Equation 11
$\Delta \rho_{inj}^{cyl}$	kg m^{-3}	Tracer gas mixture density	Primary certified cylinder	-	Equation 13
Rep_c	%	Replications of SSMRT	Standard deviation of mean SSMRP	-	Equation 16

Table 2. Pressure distribution for the six chambers at five sample locations and three heights corresponding to figure 2. Results are the average of each sample location across the three heights, and the average of the five cross-section sample locations for each of the three heights.

	Pressure (Pa; mean ±standard deviation)							
	Cross-Section Location (n = 3)[a]					Height (n = 5)[a]		
Chamber	1	2	3	4	5	Upper	Middle	Lower
1	25 ±2.1	25 ±0.9	23 ±1.7	24 ±1.4	24 ±1.1	23 ±1.5	25 ±1.4	24 ±1.1
2	23 ±3.1	22 ±3.7	22 ±3.4	20 ±1.5	19 ±0.4	22 ±3.0	23 ±2.4	18 ±0.9
3	23 ±0.9	22 ±4.1	21 ±0.4	24 ±2.7	21 ±1.2	24 ±2.2	21 ±1.1	22 ±2.6
4	20 ±2.0	21 ±3.6	22 ±6.5	20 ±2.2	17 ±2.3	17 ±1.7	22 ±3.0	21 ±3.2
5	33 ±6.7	35 ±2.0	35 ±1.6	35 ±0.6	33 ±2.2	35 ±1.8	35 ±1.2	32 ±4.3
6	19 ±0.5	19 ±2.7	17 ±1.9	17 ±2.5	20 ±0.8	17 ±2.5	19 ±1.1	19 ±1.1

[a] n = number of samples.

Bias Correction

For systematic errors found to be significant ($p < 0.05$), a correction factor can be applied to the accumulated emission (eq. 20). The effective accumulated emission was obtained from the multiplication of a correction factor (mean SSMRP fraction) by the computed accumulated emission (Maia et al., 2015):

$$E_c^{eff} = E_c \times \left(\frac{100}{\overline{\text{SSMRP}_c}} \right) \quad (20)$$

where

E_c^{eff} = effective accumulated emission measured per chamber c (g)

E_c = accumulated emission per chamber c (g; Maia et al., 2015; eq. 4).

The standard uncertainty associated with effective accumulated emission (eq. 21) combined the accumulated emission standard uncertainty (Maia et al., 2015; eq. 6) and $\Delta\overline{\text{SSMRP}_c}$ (eq. 18), yielding the following equation:

$$\Delta E_c^{eff} = \sqrt{\left(\frac{\partial E_c^{eff}}{\partial E_c} \Delta E_c \right)^2 + \left(\frac{\partial E_c^{eff}}{\partial \overline{\text{SSMRP}_c}} \Delta \overline{\text{SSMRP}_c} \right)^2} \quad (21)$$

where ΔE_c^{eff} is the standard uncertainty of effective accumulated emission per chamber c (g). If a significance test rejects the hypothesis of a system bias, the correction (eqs. 20 and 21) does not apply.

RESULTS AND DISCUSSION

SUBSYSTEM VALIDATION

The spatial distribution of static pressure inside the chambers verified chamber positive pressurization. The thermal environment performance verified the thermal environmental control system removed moisture and maintained set point temperature when the VHC was occupied with an animal. The gas sampling subsystem evaluation assessed discrepancies between the known reference gas concentration and the concentration measured with the gas analyzer. Each validation is summarized below.

Ventilated Hood Chamber Pressure Distribution

The six chambers were found to be positively pressurized for all scenarios tested (fig. 1) with values ranging from 14.5 to 37.8 Pa. The minimum value of 14.5 Pa is approximately 60 times greater than the resolution of the pressure transducer (0.25 Pa). The average and standard deviation for each sample location across the three heights and the average and standard deviation for all sample locations at each height are summarized in table 2. Visual observation of chamber flow patterns with the smoke test also confirmed positive internal pressurization. Smoke was observed to flow outward from the chamber to the room when smoke was released inside each chamber. No smoke entered the chamber when released outside of each chamber.

Table 3. Summary of dry-bulb temperatures, dew point temperatures, and humidity ratios inside the chambers with animals present for approximately 23 h.

Parameter		Chamber 1	2	3	4	5	6	Background
Temperature (°C)	Mean ±SD[a]	22.9 ±0.4	22.9 ±0.4	22.5 ±0.3	22.7 ±0.3	22.4 ±0.4	22.2 ±0.4	23.8 ±1.2
	Maximum	24.1	23.7	23.2	23.5	23.1	23	26.2
	Minimum	21.8	22.0	21.6	21.4	20.7	20.5	21.9
Dew point temperature (°C)	Mean ±SD[a]	15.7 ±0.8	14.8 ±0.9	15.9 ±0.7	15.4 ±0.6	14.6 ±0.7	15.3 ±0.7	15 ±1.1
	Maximum	17.2	17	17.2	16.8	15.9	17.2	16.6
	Minimum	13.7	12.4	13.2	12.0	10.6	13.0	11.4
Humidity ratio ($g\ H_2O\ kg^{-1}$ dry air)	Mean ±SD[a]	10.9 ±0.7	11.4 ±0.6	10.8 ±0.6	11.6 ±0.5	11.3 ±0.5	10.6 ±0.5	11.1 ±0.5
	Maximum	12.1	12.6	12.4	12.6	12.3	11.6	12.6
	Minimum	8.6	10.0	9.2	9.7	8.9	8.1	9.5

[a] SD = standard deviation

Thermal Environment Performance

Temperature for each chamber was maintained within the desired temperature range (15°C to 25°C) for adult cattle (FASS, 2010) with standard deviations of about 0.4°C. Chamber and background temperatures ranged from 20.5°C to 24.1°C and from 21.9°C to 26.2°C, respectively (fig. 5 and table 3). Chamber temperatures were influenced by diurnal patterns of background temperature. Condensation or excessive moisture has substantial negative impacts on gas concentration measurements because of potential gas sample dilution and compromised analyzer operation. The TECS was effective for moisture removal, as seen by no increase in the humidity ratio (accumulation of moisture) of chambers above the background humidity ratio; thus, moisture was constantly removed and kept below saturation (fig. 6 and table 3). The humidity ratio ranged from 8.1 to

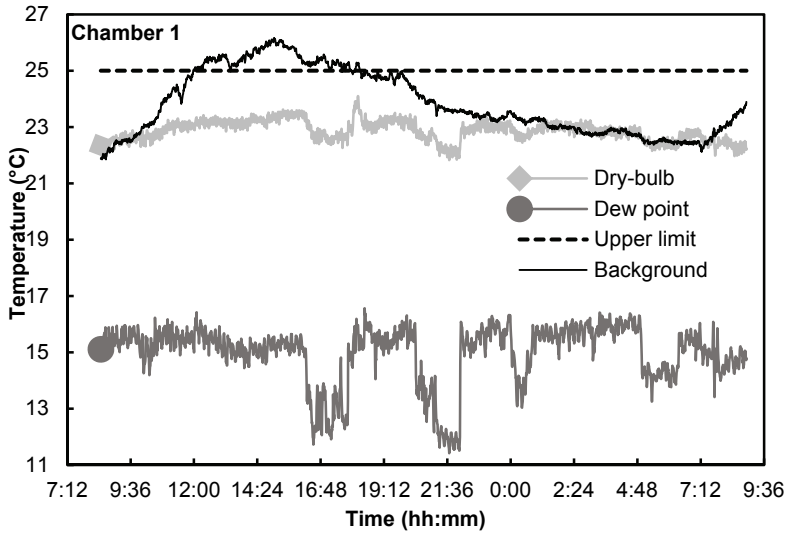

Figure 5. Example of temperature measurement over approximately 23 h for chamber 1 and the background. All chambers were maintained within the desired temperature range (upper limit of 25°C shown in figure) despite exceeding background conditions, and no condensation formed inside the chambers.

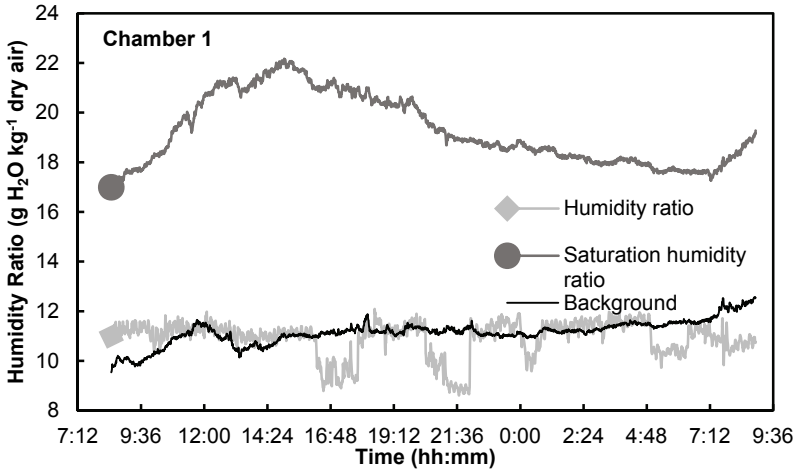

Figure 6. Example of humidity ratio from temperature and relative humidity measurement over approximately 23 h for chamber 1 and the background. All chambers adequately removed moisture generated by the animal.

Table 4. Summary of nonlinear regression (eq. 2) for four replicates (n = 4) to determine the time constant (τ) for the exchange rate of fresh air and the time to reach steady-state (5τ). Each chamber had a unique time to reach steady-state, ranging from 12.99 to 13.92 min; therefore, SSMRT analysis was conducted with gas concentration measurements after 14 min.

	Parameter (minimum - maximum)			Maximum Time to Reach Steady-State
Chamber	R^2	Regression SE (ppm_v)	τ (min^{-1})	(5τ, min)
1	0.98 - 1	0.2 - 1.2	2.2 - 2.7	13.5
2	0.98 - 1	0.1 - 1.1	2.1 - 2.8	13.9
3	0.99 - 1	0.2 - 0.9	2.2 - 2.6	13.0
4	0.98 - 1	0.1 - 1.3	2.1 - 2.7	13.4
5	0.98 - 1	0.3 - 1.0	2.3 - 2.6	13.1
6	0.99 - 1	0.1 - 1.0	2.4 - 2.7	13.7

12.6 g H_2O kg^{-1} dry air for chambers and from 9.5 to 12.6 g H_2O kg^{-1} dry air for the background. The background temperature for the duration of the test remained above the dew point temperatures (13.7°C to 15.9°C) inside the chambers; therefore, no internal condensation was formed.

Gas Sampling Subsystem Integrity

The six gas sampling paths (from each of the six chambers through the multiplexer to the gas analyzer) evaluated in the gas sampling subsystem integrity test achieved a recovery within the uncertainty of the gas analyzer (≤ ±2%). Gas sampling subsystem recoveries ranged from 100.0% to 101.4% of the expected value. Results indicated no leakage in the gas sampling path.

Steady-State Determination

The time constant for the exchange rate of fresh air in each chamber (four replicates) ranged from 2.3 to 2.5 min^{-1}, and the time for each chamber to reach steady-state (5τ) ranged from 11.6 to 12.5 min (table 4). An example nonlinear regression (eq. 2) plot for a chamber is shown in figure 7. This information established that gas concentration measurements used to calculate mass flow recovered should be made 14 min after the start of injection (a conservative estimate that ensured steady-state for all chambers).

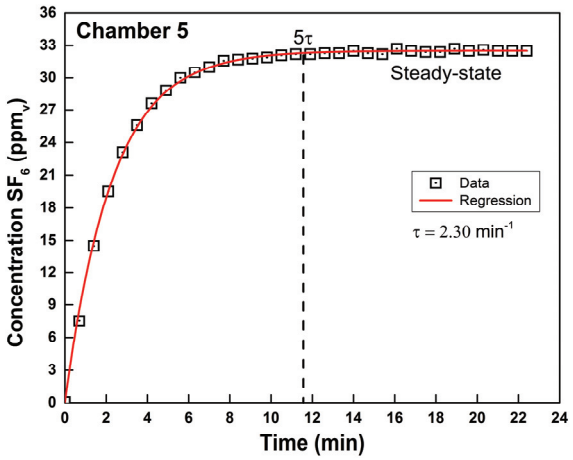

Figure 7. Example of the nonlinear regression steady-state analysis for one chamber. The solid line is the nonlinear regression (eq. 2) fitted to the measured concentrations(data). Five time constants (5τ) were used as a conservative estimate for determining the time to steady-state (<14 min for all chambers).

Overall uncertainty for the regression was quantified with the regression standard error (SE). The SE of each coefficient (i.e., τ) provides information about the overall uncertainty associated with the computation of the time constant. In addition, the average coefficients of determination (R^2) were greater than 0.99 for the nonlinear regression applied to equation 2.

The time to reach steady-state was used to improve experimental and operational protocols. For example, gas sampling should not begin until chamber conditions reach steady-state (i.e., after 14 min). Once gas concentration profile patterns are stable, changes in CH_4 generation can be estimated. For REMS, injected gas should be allowed to mix undisturbed for at least 14 min prior to using gas concentration measurements for analysis. In addition, if the chamber is opened during an experiment, gas concentration measurements must be discarded until the gas inside the chamber has returned to steady-state.

Four hours were required to perform a complete steady-state recovery analysis for the six chambers. In addition, one SF_6 primary certified tank can be used to complete 24 mass recovery tests. Alternative methods of mass recovery tests, such as gas release from a cylinder on a scale or single-volume gas injection from a canister, can take 4 to 24 h to complete (Hellwing et al., 2012; Williams et al., 2007) and require a larger volume of gas.

Steady-State Mass Recovery Analysis

The mean SSMRP for the six chambers ranged from 92.0% (chamber 3) to 96.6% (chamber 6) (table 5). The reproducibility (standard deviation of the SSMRP mean) for each chamber ranged from 1.3% (chamber 5) to 3.2% (chamber 4). The technical literature has recommended recoveries of 95% to 105% for newly constructed respiration chambers (Suzuki et al., 2007), or an extensive evaluation should be conducted to attain 100% recovery (McLean and Tobin, 1987). Equally important, however, is the systematic quantification and documentation of the uncertainties and bias associated with the recovery test. Lower recovery, such as measured here, can be attributed to several factors, including gas sampling system leakage, measurement errors, and non-ideal mixing inside the chamber. The commissioning suggests that GSS leakage and infiltration in the chamber can be excluded as a cause of lower recovery because the GSS underwent a comprehensive and systematic evaluation of leaks, and the chamber was verified as a positively pressurized low-leak system. Second, instrument measurement error has been exhaustively covered (Maia et al., 2015) and is less than the apparent bias observed. Non-ideal mixing patterns could occur from short-circuiting of the injected gas inside the chamber. While that might be a cause for recoveries lower than 95% in this work, the high reproducibility of the recoveries further indicate a consistent bias. For these cases, systematic errors can be corrected following the previously described methods.

A correction factor may be applied in the event that recovery percent is not improved and is different from 100% (McLean and Tobin, 1987). McGinn et al. (2004) created correction factors accounting for between-chamber differ-

Table 5. Summary of mass recovered by each chamber, mass injected by the reference, and the mean SSMRP for eight replicates.

	Parameter (minimum - maximum)		
Chamber	Mass Recovered (g)	Mass Injected (g)	$\overline{SSMRP}$ ±Rep[a] (%)
1	0.7 - 1.0	0.8 - 1.1	93.2 ±1.7
2	0.8 - 1.0	0.8 - 1.1	94.9 ±1.6
3	0.7 - 1.0	0.8 - 1.1	92.0 ±2.2
4	0.7 - 1.0	0.8 - 1.1	92.8 ±3.2
5	0.8 - 1.1	0.8 - 1.1	94.3 ±1.3
6	0.8 - 1.1	0.8 - 1.1	96.6 ±1.4

[a] Rep = reproducibility (eq. 16).

Table 6. Absolute (Abs.) and relative (Rel.) standard uncertainties for mass recovered and mass injected. The range of absolute standard uncertainties for SSMRP is also reported.

	Combined Standard Uncertainty (minimum - maximum)				
	Mass Recovered		Mass Injected		
Chamber	Abs. (g)	Rel. (%)	Abs. (g)	Rel. (%)	ΔSSMRP (%)
1	<0.06	5.2 - 5.3	<0.01	1.1	5.2 - 5.4
2	<0.06	5.5 - 5.5	<0.01	1.1	5.4 - 5.7
3	<0.06	5.3 - 5.3	<0.01	1.1	5.4 - 5.7
4	<0.06	5.7 - 5.7	<0.01	1.1	6.2 - 6.5
5	<0.06	5.3 - 5.5	<0.01	1.1	5.2 - 5.4
6	<0.06	5.2 - 5.2	<0.01	1.1	5.2 - 5.5

ences in order to increase treatment sensitivity. Using three replicated mass recovery tests during the course of an experiment, a correction factor for each chamber was obtained from the ratio of the maximum recovery to the other chambers' recovery (McGinn et al., 2004). However, the development, validity, and consequence of these correction factors are scarcely documented, and what is reported does not include detailed experimental and analytical procedures to determine mass recovery percent and its associated standard deviation (i.e., standard deviation of replicates or of the set of chambers; Ramirez, 2014). An approach to correct for consistently lower recoveries such as encountered here was implemented to include reproducibility in the calculation of the mean SSMRP standard uncertainty (eqs. 17 and 18).

STANDARD UNCERTAINTY FOR STEADY-STATE MASS RECOVERY

Standard uncertainty associated with the mass of recovered and injected tracer gas and their ratio (SSMRP) are reported in table 6. All six chambers exhibited a standard uncertainty of mass recovered of <0.06 g SF_6 (table 6), or less than 6.0% on a relative basis. Prior to integration over the steady-state test period, mass flow recovered standard uncertainty was similar to that reported for emission rate standard uncertainty (Maia et al., 2015). This was expected because the individual sources for uncertainty in the mass flow recovery and the uncertainties associated with these sources were equivalent to those used to determine the uncertainties associated with emission rates. Mass injected standard uncertainty was the same for all six chambers (<0.01 g of SF_6) with a relative standard uncertainty of 1.1% for all chambers and all replicates.

Contributions from Mass Flow Recovered

For all six chambers, ventilation rate contributed the most to the mass flow recovered standard uncertainty, with contributions ranging from 48.3% (chamber 1) to 60.3% (chamber 4) (fig. 8). Concentration measurement during steady-state was the second highest contributor, ranging from 32.8% (chamber 4) to 42.1% (chamber 1), followed by background concentration measurement, which ranged from 5.5% (chamber 4) to 8.0% (chamber 3) (fig. 8). Absolute standard uncertainties of ventilation rate measurement (Ramirez, 2014; Ramirez et al., 2014) and concentration measurement (Maia et al., 2015) are discussed elsewhere. Remaining sources (chamber and background temperature, density, and injected flow) totaled less than 3.0% for all chambers and all replicates. Although the background mass of SF_6 was not neglected in this analysis, it had a minimal effect on the overall standard uncertainty because SF_6 background concentrations were close to zero. The decision to maintain SF_6 background concentrations in the recovery model was retained so that this methodology may be extended to other candidate gases for which background concentrations are substantially present and variable (i.e., CO_2 or CH_4).

Contributions from Mass Flow Injected

For all six chambers, injected tracer gas flow uncertainty contributed the most to the mass flow injected standard

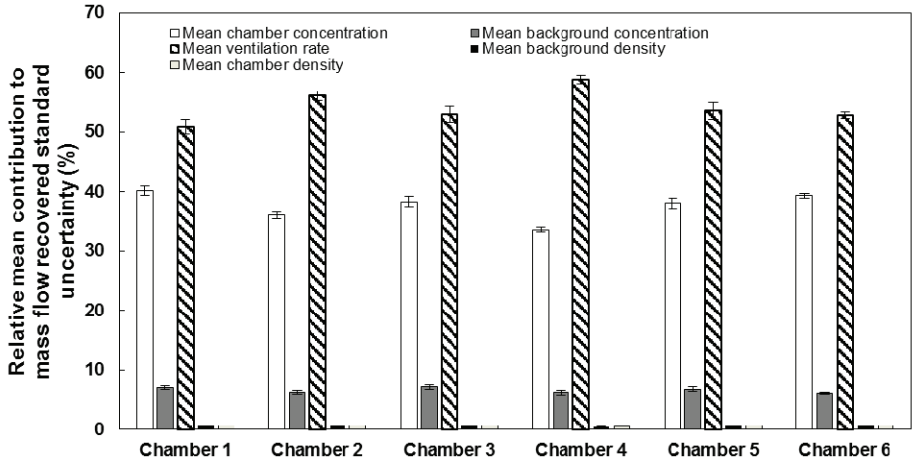

Figure 8. Relative mean contribution to mass flow recovered standard uncertainty averaged for all replicates. Error bars represent standard deviations obtained by replicates. Other parameters are omitted for clarity and had <3% contribution. Major contributions from ventilation rate and concentration measurement were consistent across all the six chambers.

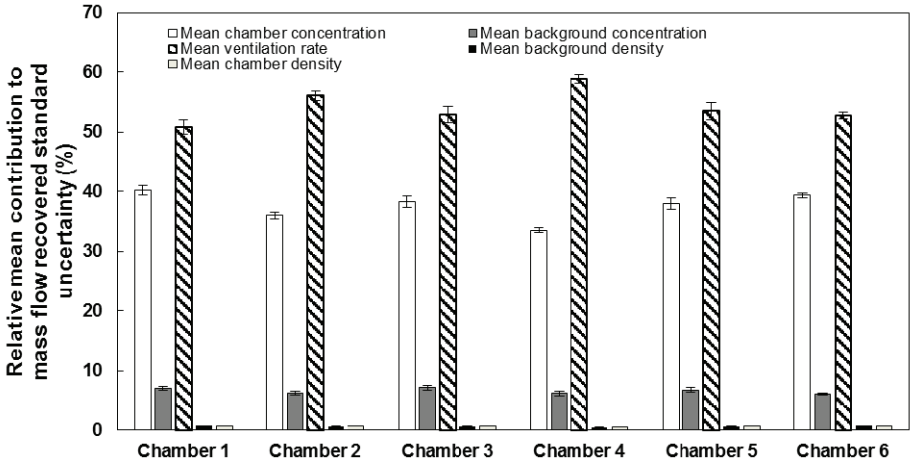

Figure 9. Relative mean contribution to mass flow injected standard uncertainty averaged for all replicates. Standard deviations obtained by replicates were much less than 1%. Injected flow contributed approximately 91% to mass flow injected standard uncertainty.

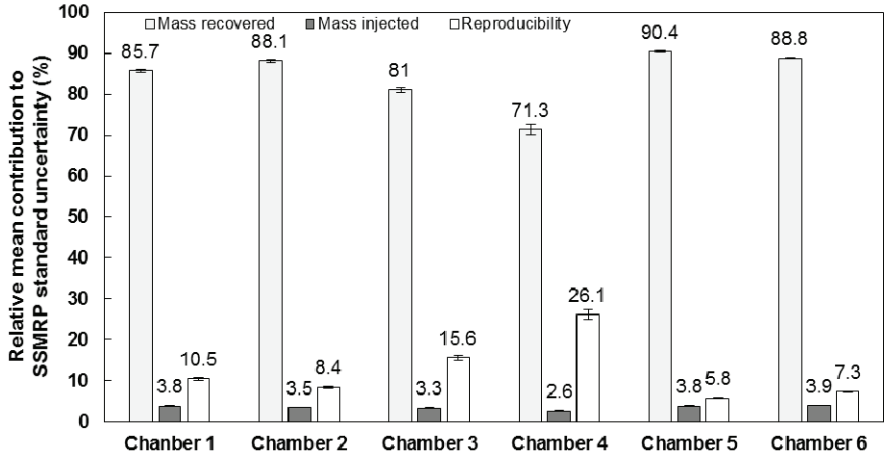

Figure 10. Mean relative contribution to steady-state mass recovery percent (SSMRP) standard uncertainty for all replicates. Error bars represent standard deviations for replicates (n = 8). Mass recovered had the greatest contribution, while the contribution of reproducibility was positively correlated with its magnitude.

uncertainty (91.0%; fig. 9). The remaining 9.0% contributing to mass flow injected standard uncertainty was uncertainty related to injected concentration. This illustrates the importance of having an accurate and stable mass flow controller or other source of constant gas injection.

Contributions from SSMRP

The three major sources of uncertainty in SSMRP for each chamber (mass injected, mass recovered, and reproducibility) were assessed in terms of their relative contribution to overall SSMRP uncertainty. Mass recovered uncertainty contributed from 70.1% (chamber 4) to 90.7% (chamber 5) to SSMRP standard uncertainty, while mass injected uncertainty contributed from 2.5% (chamber 4) to 4.0% (chamber 6; fig. 10). The small contribution of the reference mass injected was due to the use of accurate instrumentation and gas certification, which highlights the importance of providing detailed uncertainty information for the reference mass to improve confidence in recovery results. Reproducibility had a small but substantial contribution, ranging from 5.6% (chamber 5) to 27.3% (chamber 4), to the SSMRP standard uncertainty (fig. 10), which reflects qualified personnel operating the system combined with regular instrument drift checks and calibration. By reducing the uncertainty in the major sources identified here, such as ventilation rate and gas concentration measurement, the SSMRP standard uncertainty can also be decreased.

Bias Evaluation for Accumulated Emissions

Systematic errors (bias) were significant ($p < 0.05$) for chambers 1 through 5, as summarized in table 7. Bias correction is hence recommended for chambers 1 through 5 (eqs. 21 and 22) and not needed for chamber 6. Note that as new experiments are performed, correction factors used to

Table 7. Inference testing to determine chambers biases using eight replicates of the SSMRT over one year.

	Chamber					
Parameter	1	2	3	4	5	6
$\overline{SSMRP}_c$ (%)	93.2	94.9	92.0	92.8	94.3	96.6
$\Delta\overline{SSMRP}_c$ (%)	1.9	2.0	2.0	2.2	1.9	1.9
p-Value	0.009	0.037	0.005	0.015	0.019	0.113
Bias?[a]	Yes	Yes	Yes	Yes	Yes	No

[a] Bias correction is recommended for chambers 1 through 5 (eqs. 21 and 22) and not recommended for chamber 6.

Table 8. Sample accumulated CH_4 emissions and associated standard uncertainty calculation for six steers fed grain and forage diets. Correction factors and their associated standard uncertainty were applied to accumulated emissions data for chambers 1 through 5.

Chamber	Animal	Body Weight (kg)	Diet	$E \pm \Delta E$ (g d^{-1})[a]	Relative ΔE (%)	Correction Factor	$E^{eff} \pm \Delta E^{eff}$ (g d^{-1})[b]	Relative ΔE^{eff} (%)
1	A	922.6	Forage	75.59 ±8.72	11.53	1.07	81.07 ±9.49	11.71
		982.0	Grain	43.56 ±5.80	13.31		46.71 ±6.29	13.46
2	B	740.3	Forage	112.36 ±9.85	8.77	1.05	118.34 ±10.66	9.01
		793.8	Grain	110.22 ±9.19	8.34		116.10 ±9.98	8.59
3	C	787.0	Forage	109.09 ±8.38	7.68	1.09	118.56 ±9.44	7.96
		862.3	Grain	105.31 ±7.34	6.97		114.46 ±8.33	7.28
4	D	782.9	Forage	69.69 ±7.34	10.54	1.08	75.07 ±8.11	10.81
		771.1	Grain	74.06 ±6.65	8.97		79.79 ±7.41	9.29
5	E	904.0	Forage	74.79 ±5.81	7.77	1.06	79.32 ±6.36	8.02
		879.5	Grain	106.37 ±8.66	8.14		112.80 ±9.46	8.38
6	F	882.7	Forage	119.26 ±7.65	6.42	-	-	-
		843.2	Grain	123.22 ±8.14	6.60		-	-

[a] Accumulated emissions with standard uncertainty reported (Maia et al., 2015; eq. 4).
[b] Effective accumulated emissions from application of correction factor (eq. 20) with standard uncertainty reported (eq. 21).

Table 9. Methane emissions as a proportion of dry matter intake (DMI) before and after bias correction. Each animal was placed in REMS for two different diets (forage and grain) for 24 h each in different periods.

Animal	Diet	GS[a] DMI (kg d^{-1})	REMS[b] DMI (kg d^{-1})	Methane Emissions (g CH_4 kg^{-1} DMI d^{-1}) Uncorrected	Bias Corrected
A	Forage	14.6	6.0	7.2	7.8
	Grain	15.9	0.9[c]	86.4	92.7
B	Forage	11.3	8.1	13.6	14.3
	Grain	12.8	6.0	18.9	19.9
C	Forage	10.8	7.0	15.1	16.4
	Grain	13.5	7.3	14.9	16.2
D	Forage	7.8	6.0	12.3	13.2
	Grain	11.6	8.0	8.7	9.4
E	Forage	12.1	6.2	17.0	18.1
	Grain	16.7	10.3	7.3	7.7
F	Forage	8.9	4.2	29.3	n.a.
	Grain	12.9	6.6	18.2	n.a.

[a] Dry matter intake within a GrowSafe (GS) environment (average DMI ten days prior to transfer of animals to REMS). Data source for DMI values: Lehman et al. (2014).
[b] Dry matter intake while animal was in REMS. A lower intake was observed for animals inside the chamber, as previously reported (Freetly and Brown-Brandl, 2013). Additional training might be required before animals are exposed to treatment in REMS.
[c] Animal did not consume food in the chamber.

calculate the effective accumulated emissions should be updated, pending the results of new SSMRTs.An example of the calculated accumulated emissions and standard uncertainty is presented in table 8 for the six chambers. The data provided in table 8 were obtained from six large steers placed in the chambers for approximately 24 h. Values from chambers 1 through 5 were corrected for systematic errors, and their corresponding effective emissions were determined.

For all six chambers, as the accumulated emissions increased, the relative standard uncertainty decreased. This result was similar to the result found in the ER sensitivity analysis documented in Part I (Maia et al., 2015). The effective accumulated emissions and associated standard uncertainty increased after application of the systematic error correction (eqs. 20 and 21) for chambers 1 through 5. Methane emissions as a proportion of body weight and dry matter intake (BMI) are provided in table 9.

Analysis of the effects of different treatments on CH_4 emissions is beyond the scope of this work; however, there are important implications relative to using the methods presented here. For example, the sources of measurement errors combined into the emission standard uncertainty (corrected or uncorrected) are rarely used in a means comparison to evaluate the effects of, e.g., diet, management, or genetics on CH_4 production. Consequently, treatment effects are often found to be significant because measurement errors are not accounted for. Alternatively, treatment effects detected by REMS have a high probability of representing real effects. REMS is a major contribution toward the integration of measurement system uncertainty analysis into statistical design.

SUMMARY AND CONCLUSIONS

In commissioning REMS, its subsystems were individually evaluated, followed by a whole-system evaluation via SSMRT analysis. The SSMRT analysis included REMS steady-state determination, the steady-state mass recovery ratio expressed on a percent basis (SSMRP), and the relative contributions of individual sources of uncertainty to the SSMRP uncertainty.

Subsystem evaluation: Results of the subsystem evaluation showed that the six chambers were positively pressurized, maintained a suitable thermal environment, and had no leakage along the sampling path from the chamber to the gas analyzer. No obvious errors or malfunctions were found; therefore, any loss of mass indicated by the SSMRT was due to other sources of errors than the ones found in the subsystem assessment.

Steady-state mass recovery test: The SSMRT analysis quantified the degree of mass conservation detected by REMS. It served as a whole-system verification, identified random and systematic errors, and determined the time constant for the exchange rate of fresh air in each chamber.

Steady-state determination: Steady-state operation was quantified and was achieved within 14 min for all six chambers (five time constants). A mathematically determined time constant provides insight into chamber mixing patterns, which improves the development of experimental and operational procedures and protocols. Changes in the time constants over time are a useful metric to identify sys-

tem drift or other problems.

Steady-state mass recovery percent: REMS mass conservation was assessed as the ratio between the total mass recovered by REMS and a precisely metered amount of mass injected by the reference. Mean SSMRP for the six chambers ranged from 92.0% (chamber 3) to 96.6% (chamber 6) with a reproducibility ranging from 1.3% (chamber 5) to 3.2% (chamber 4). The SSMRP absolute expanded uncertainty (k = 2, ~95% C.I.) ranged from 10.4% (chambers 1, 5, and 6) to 13.0% (chamber 4) and accounted for individual instrument measurement uncertainties, mass recovered uncertainty, mass injected uncertainty, and reproducibility.

Individual uncertainty relative contributions: SSMRP uncertainty relative contributions ranged from 70.1% (chamber 4) to 90.7% (chamber 5) for mass recovered, from 2.5% (chamber 4) to 4.0% (chamber 6) for mass injected, and from 5.6% (chamber 5) to 27.3% (chamber 4) for recovery test reproducibility. Uncertainties related to the orifice meter and gas analyzer were the two major sources of uncertainty for the mass recovered, with the orifice meter being the highest. These two uncertainty sources were analyzed in detail for REMS emission rates in Part I (Maia et al., 2015). The mass flow controller was the major source of uncertainty for the injected reference mass.

Systematic error: Significant systematic errors were detected in the SSMRT analysis for chambers 1 through 5. A correction (eq. 20) is recommended for accumulated emissions calculated from these chambers.

While this analysis was applied to only REMS, it applies equally to any open-circuit respiration chamber or, by appropriate measurements, to indirect calorimetry. Confidence in a measurement system is strongly dependent on the quality of the information obtained from instrument resolution, reproducibility, calibration reference standard error, other calibration parameters, and manufacturers' traceable and non-traceable accuracy. Integration of these sources of uncertainty and development of an expanded standard uncertainty using coverage factors provides confidence intervals for operation and emission measurements. In addition, analysis of the relative contributions of individual uncertainty sources to overall system uncertainty should be performed, along with the assessment and correction (if applicable) of system systematic errors. In conclusion, a comprehensive analysis of measurement uncertainty should be an integral part of the experimental design of any open-circuit respiration system constructed to study the effects of different treatments on ruminant emissions.

ACKNOWLEDGEMENTS

This research was supported with funding provided by the Dudley Smith Initiative, University of Illinois College of ACES, and the Office of Research, University of Illinois College of ACES. The authors would like to acknowledge the contributions of research specialist Jingwei Su, graduate students Jacob Segers and Blake Lehman, and undergraduate students Kellie Kroscher and Patricia Paulausky during the preparation and completion of this work.

REFERENCES

Albright, L. D. (1990). *Environment Control for Animals and Plants.* St. Joseph, Mich.: ASAE.

ASHRAE. (2013). Chapter 1: Psychrometrics. In M. S. Owen (Ed.), *Handbook of Fundamentals.* Atlanta, Ga: ASHRAE.

Carpenter, T. M., & Fox, E. L. (1923). Alcohol check experiments with portable respiration apparatus. *Boston Med. Surgical J., 189*(16), 551-561. http://dx.doi.org/10.1056/NEJM192310181891602.

FASS. (2010). Guide for the care and use of agricultural animals in research and teaching. Champaign, Ill.: Federation of Animal Science Societies. Retrieved from www.fass.org/docs/agguide3rd/Ag_Guide_3rd_ed.pdf.

Freetly, H. C., & Brown-Brandl, T. M. (2013). Enteric methane production from beef cattle that vary in feed efficiency. *J. Animal Sci. 91*(10), 4826-4831.

Gates, R. S. (1994). Dew point temperature error from measuring dry bulb temperature and relative humidity. *Trans. ASAE, 37*(2), 687-688. http://dx.doi.org/10.13031/2013.28130.

Gates, R. S., Casey, K. D., Xin, H., & Burns, R. T. (2009). Building emissions uncertainty estimates. *Trans. ASABE, 52*(4), 1345-1351. http://dx.doi.org/10.13031/2013.27784.

Hellwing, A. L. F., Lund, P., Weisbjerg, M. R., Brask, M., & Hvelplund, T. (2012). Technical note: Test of a low-cost and animal-friendly system for measuring methane emissions from dairy cows. *J. Dairy Sci., 95*(10), 6077-6085. http://dx.doi.org/10.3168/jds.2012-5505.

ISO/IEC. (2008). ISO/IEC Guide 98-3: Uncertainty of measurement —Part 3: Guide to the expression of uncertainty in measurement (GUM:1995). Geneva, Switzerland: International Standards Organization.

Jordan, K. A., Kuehl, R.O., & Sewell, J. I. (1991) Chapter 1: Planning the experiment. In Z. A. Henry, G. C. Zoerb, and G. S. Birth (Eds.), *Instrumentation and Measurements for Environmental Sciences* (3rd Ed.). St. Joseph, Mich.: ASAE.

Klein, L., & Wright, A. G. (2006). Construction and operation of open-circuit methane chambers for small ruminants. *Australian J. Exp. Agric., 46*(10), 1257-1262. http://dx.doi.org/10.1071/EA05340.

Lehman, B., Green, A. R., Felix, T. L., Ramirez, B. C. Rodriguez, L. F., & Shike, D. W. (2014). Effects of diet on intake and methane emissions of beef steers. In *Proc. ADSA-ASAS Midwest Meeting*. Champaign, Ill.: American Society of Animal Science.

Maia, G. D. N., Ramirez, B. C., Green, A. R., Rodriguez, L. F., Segers, J. R., Shike, D. W., & Gates, R. S. (2015). A novel ruminant emission measurement system: Part I. Design evaluation and description. *Trans. ASABE., 58*(3), 749-762.

McGinn, S. M. (2006). Measuring greenhouse gas emissions from point sources in agriculture. *Canadian J. Soil Sci., 86*(3), 355-371.

McGinn, S. M., Beauchemin, K. A., Coates, T., & Colombatto, D. (2004). Methane emissions from beef cattle: Effects of monensin, sunflower oil, enzymes, yeast, and fumaric acid. *J. Animal Sci., 82*(11), 3346-3356.

McLean, J., & Tobin, G. (1987). *Animal and Human Calorimetry.* Cambridge, U.K.: Cambridge University Press.

Pinares-Patiño, C. S., Lassey, K. R., Martin, R. J., Molano, G., Fernandez, M., MacLean, S. E., Sandoval, E., Luo, D., & Clark, H. (2011). Assessment of the sulphur hexafluoride (SF_6) tracer technique using respiration chambers for estimation of methane emissions from sheep. *Animal Feed Sci. Tech.*, 166-167, 201-209. http://dx.doi.org/10.1016/j.anifeedsci.2011.04.067.

Ramirez, B. C. (2014). Design and evaluation of open-circuit respiration chambers for beef cattle. MS thesis. Urbana, Ill.: University of Illinois at Urbana-Champaign, Department of Agricultural and Biological Engineering.

Ramirez, B. C., Maia, G. D. N., Green, A. R., Rodriguez, L. F., Shike, D. W., & Segers, J. R. (2014). Design and validation of a precision orifice meter for sub-550 liter per minute flow rate applications. *Trans. ASABE, 57*(6), 1865-1872. http://dx.doi.org/10.13031/trans.57.10754.

Sun, Y. (2013). Quality assurance project plan for a ruminant emission measurement system. MS thesis. Urbana, Ill.: University of Illinois at Urbana-Champaign, Department of Agricultural and Biological Engineering.

Suzuki, T., McCrabb, G., Nishida, T., Indramanee, S., & Kurihara, M. (2007). Construction and operation of ventilated hood-type respiration calorimeters for *in vivo* measurement of methane production and energy partition in ruminants. In *Measuring Methane Production From Ruminants* (pp. 125-135). Dordrecht, The Netherlands: Springer. http://dx.doi.org/10.1007/978-1-4020-6133-2_8.

Taylor, B. N., & Kuyatt, C. E. (1994). Guidelines for evaluating and expressing the uncertainty of NIST measurement results. NIST Technical Note 1297. Gaithersburg, Md.: National Institute of Standards and Technology.

Williams, Y. J., Klein, L., & Wright, A.-D. G. (2007). A protocol for the operation of open-circuit chambers for measuring methane output in sheep. In H. P. Makkar, & P. E. Vercoe (Eds.), *Measuring Methane Production from Ruminants* (pp. 111-123). Dordrecht, The Netherlands: Springer. http://dx.doi.org/10.1007/978-1-4020-6133-2_7.

Zhang, Y. (2005). *Indoor Air Quality Engineering.* Baco Raton, Fla.: CRC Press.